Kinetic and Energetic Analysis of the Free Electron Transfer

Aliaksandr Baidak,[†] Sergej Naumov,[‡] and Ortwin Brede*,[†]

Interdisciplinary Group Time-Resolved Spectroscopy, University of Leipzig, Permoserstrasse 15, 04303 Leipzig, Germany, and Leibniz Institute of Surface Modification, Permoserstrasse 15, 04303 Leipzig, Germany

Received: June 19, 2008; Revised Manuscript Received: July 29, 2008

In this paper, the bimolecular free (unhindered) electron transfer (FET) from various trityl-containing compounds to the solvent radical cations of *n*-BuCl is described. In good agreement with the previously studied cases, the FET involving trityl-derived compounds results in the formation of two different types of the radical cation, which undergo the subsequent fragmentation via two alternative reaction channels. This unusual effect is caused by the intramolecular rotational motion in the ground-state molecules around the arrow-marked bond Ar-↷-X-CPh_3 (Ar = aromatic moiety; X = S, O, NH, CH_2), since such oscillations are directly connected with the electron distribution within the molecule. An unhindered electron jump from the donor trityl compound to the solvent radical cation, taking place in the subfemtosecond time range, generates the solute radical cation with the inherited geometry and the electron distribution of its precursor. Among the whole variety of produced radical cations, two extreme conformer states can be distinguished, namely, a planar and a twisted state. The planar type represents the structures with minimum energy, whereas the twisted type is destabilized by the increased value of the rotational barrier in the ionized state. The difference in the energetic profiles between planar and twisted radical cations plays a crucial role in their subsequent fragmentation. The planar radical cation follows the thermodynamically favored pathway generating $ArX^{\bullet}$ and Ph_3C^+. A distinct part of the twisted radical cation dissociates faster than it relaxes into the more preferable planar conformation and, therefore, produces a thermodynamically unfavorable couple of products: ArX^+ and $Ph_3C^{\bullet}$. This fragmentation channel is exclusively caused by FET. The undertaken quantum chemical calculations enable the judgment of the energetics of the different dissociation channels of the radical cations of the trityl derivatives.

Introduction

For decades, it has been known that the parent radical cations formed in the radiolysis of alkanes[1] and alkyl chlorides[2] act as extremely efficient electron acceptors toward a large variety of organic donor molecules. This bimolecular one-electron oxidation in nonpolar media proceeds in a diffusion-controlled manner and is usually called free electron transfer[3] (FET) in the sense of an unhindered transfer, cf. eqs 1a and 1b.

$$\text{RX-e-beam} \rightarrow RX^{\bullet+} + e^-_{solv}\text{, radicals, etc.} \quad X = H, Cl \tag{1a}$$

$$RX^{\bullet+} + D \rightarrow RX + D^{\bullet+} \quad D = \text{donor molecule} \tag{1b}$$

Experimentally, the FET reaction appears as an intriguing and, at first glance, surprising phenomenon. It has to do with the fact that for a large number of donor systems (phenols,[4,5] thiophenols,[6] aromatic amines,[7,8] naphthols,[9] and aromatic silanes[10,11]) the free electron transfer (eq 1b) results in the prompt formation of two distinguishable products. Hence, for such heteroatom-substituted electron donors the parallel formation of two different FET products is observed, namely, the metastable solute radical cations as well as corresponding solute-derived radicals (see Scheme 1).

This experimental fact has been interpreted to be a result of the femtosecond intramolecular dynamics, which, however, is reflected on the nanosecond time scale. Indeed, in the femtosecond time range the donor molecules exhibit pronounced bending and vibrational motions of the substituents, creating a dynamic mixture of rotational conformers. Aforementioned intramolecular motions are connected with the changes of the electron distribution in the molecule. Rapid ionization of these different conformer states takes place as an unhindered electron jump (≤1 fs) in the first encounter of the reactants. Thus, in the very beginning two types of the donor radical cations are formed, i.e., a metastable and a dissociative one; see Scheme 1. The donor radical cations in the planar state exhibit the resonant electron distribution whereas the twisted conformers demonstrate more pronounced spin localization at the heteroatom. This fact determines the very different stability of these two types of conformers, since the metastable planar radical cation is living long enough to be detected with the nanosecond technique, whereas the dissociative twisted radical cation deprotonates immediately.

SCHEME 1: Mechanism of the FET on the Example of Phenol[a]

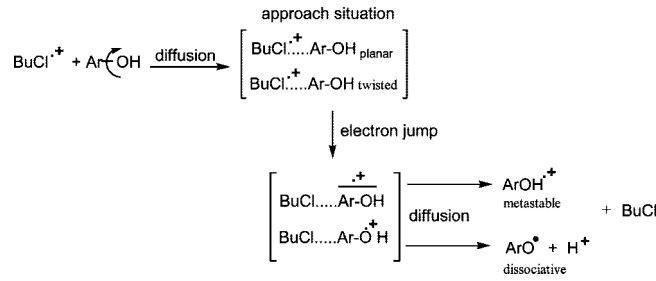

[a] The formation of two extreme conformer donor radical cations with different stabilities is shown.

* Corresponding author. brede@mpgag.uni-leipzig.de.
[†] University of Leipzig.
[‡] Leibniz Institute of Surface Modification.

10.1021/jp8053982 CCC: $40.75 © 2008 American Chemical Society
Published on Web 09/13/2008

CHART 1: List of Compounds Used

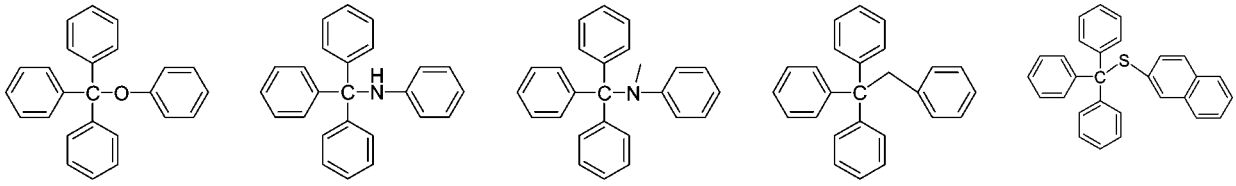

The influence of the short living conformers on the product pattern in FET, described here on example of phenol, has been clearly observed for a large variety of other donor molecules consisting of an aromatic moiety and a substituent that was able to exhibit considerable bending motions toward the aromatic ring. The special properties of the FET were characterized in detail in a feature article in this journal.[3]

More than a century ago, Gomberg was the first to report the stable trityl (triphenylmethyl) radical.[12] In his later work, triarylmethyl halides were shown to be a convenient source of stable carbocations.[13] In the case of the triarylmethyl systems, conversions among all three species (cation, radical, and anion) proceed easily upon changing of acidic−basic properties of the solvent.[14]

The purpose of this paper is to demonstrate how the advantageous properties of trityl-containing aromatic compounds (trityl moiety is a good leaving group; trityl transients are easily detected and quantitatively characterized by means of time-resolved spectroscopy) are used for the exploration of the mechanistic aspects of the FET.

Experimental Section

Pulse Radiolysis. A pulse transformer electron accelerator ELIT (Institute of Nuclear Physics, Novosibirsk, Russia) was used for irradiation of the liquid samples with high-energy electron pulses (1 MeV, 15 ns pulse duration). The solutions, purged with nitrogen or oxygen, were permanently passed though the quartz sample cell (1 cm length). The absorbed dose per pulse was estimated to be around 100 Gy measured by absorption of the solvated electron in aqueous solution. The optical detection system includes a pulsed xenon lamp (XBO 450, Osram), a Spectra Pro-500 monochromator (Acton Research Corporation), a R9220 photomultiplier (Hamamatsu Photonics), and a 1 GHz digitizing oscilloscope (TDS 640, Tektronix). All the measurements were performed in freshly prepared *n*-butyl chloride solutions. All the experiments were carried out at room temperature.

Chemicals. All chemicals and solvents necessary for the synthesis of compounds listed in Chart 1 were purchased from Sigma-Aldrich, Fluka, and Merck.

2-Naphthyltriphenylmethyl sulfide 2-NpSCPh$_3$ was obtained by reaction of 2-thionaphthol and triphenylchloride under reflux in benzene solution according to the preparation procedure described for triphenylmethyl phenyl sulfide.[15] Triphenylmethyl phenyl oxide PhOCPh$_3$ was synthesized by coupling of Ph$_3$CCl with PhONa in dry ether under reflux for 4 h.[16] Triphenylmethyl phenyl amine PhNHCPh$_3$ was prepared as described by Siskos et al.[17] Synthesis of *N*-methyl-*N*-triphenylmethyl aniline PhN(Me)CPh$_3$ followed the method introduced by Behloul et al.[18] Preparation of 1,1,1,2-tetraphenylethane PhCH$_2$CPh$_3$ was made by coupling of Ph$_3$CLi and PhCH$_2$Br in absolute THF at low temperature.[19]

All prepared compounds were recrystallized 2−3 times from clean solvents (usually ethanol or its mixtures with other organic solvents). For purification of PhOCPh$_3$ and PhN(Me)CPh$_3$, column chromatography was used. Products were characterized with ^{1}H and ^{13}C NMR techniques. Their melting points were identical to the values given in the literature.

Results

Pulse Radiolysis of 2-Naphtyl Triphenylmethyl Sulfide. Studies on the FET involving some aromatic sulfides were already reported in the literature.[20] In the case of triphenylmethyl phenyl sulfide (PhSCPh$_3$), the ionization in nonpolar media results in the appearance of two couples of fragmentation products. Thus, the formation of the triphenylmethyl radical Ph$_3$C$^\bullet$ and the triphenylmethyl cation Ph$_3$C$^+$ has been observed, while the counter fragments derived from phenyl part of the molecule have not been detected, probably due to their low extinction coefficients. The lifetime of the initial radical cation derived from PhSCPh$_3$ was found to be very short, i.e., ≤25 ns.

Therefore, it was tempting to carry out pulse radiolysis experiments with compounds possessing larger aromatic moiety, such as 2-naphthyltriphenylmethyl sulfide (2-NpSCPh$_3$). Due to the extended aromatic system, 2-NpSCPh$_3$ was expected to create more stable radical cations, which could be directly observed.

Figure 1 shows spectra obtained during pulse radiolysis of 2 × 10^{-3} molar solution of 2-NpSCPh$_3$ in *n*-butyl chloride.

The spectrum of the transients derived from 2-naphthyltriphenylmethyl sulfide taken 45 ns after the electron pulse exhibits three pronounced absorption bands at 335 nm, 420−440 nm and a broadband between 550 and 750 nm with λ_{max} about 660 nm (cf. Figure 1). Additionally, a shoulder at 500 nm is observed.

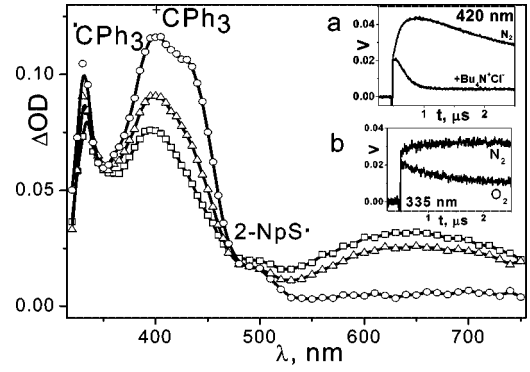

Figure 1. Transient optical absorption spectra obtained in the pulse radiolysis of N_2-saturated solution of 2-NpSCPh$_3$ (2 × 10^{-3} mol dm^{-3}) in BuCl. Spectra correspond to times (□) 45 ns, (Δ) 140 ns, (○) 700 ns after the pulse. Experimental time profiles demonstrating the influence of $Bu_4N^+Cl^-$ (a) and O_2 (b) on kinetic behavior of the transients are given as insets.

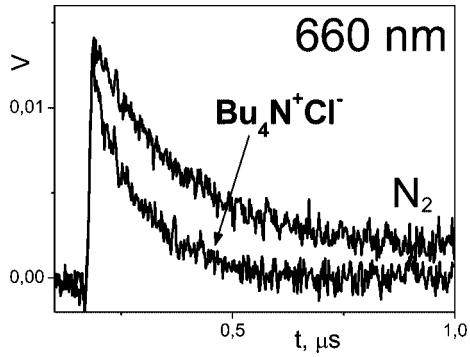

Figure 2. Experimental time profiles obtained during pulse radiolysis of N_2-saturated solution of 2×10^{-3} mol dm^{-3} 2-NpSCPh$_3$ in *n*-butyl chloride at 660 nm in the absence and presence of 4×10^{-4} mol dm^{-3} $Bu_4N^+Cl^-$.

The absorption band at 335 nm was attributed to the trityl radical $Ph_3C^{\bullet}$.[21] This carbon-centered radical is quenched by oxygen with $k_2 = (9 \pm 1) \times 10^8$ dm^3 mol^{-1} s^{-1} (cf. eq 2) and inset b in Figure 1).

$$Ph_3C^{\bullet} + O_2 \rightarrow Ph_3COO^{\bullet} \quad (2)$$

The intense absorption band at 420−440 nm was assigned to the trityl cation Ph_3C^+.[22] As expected, this charged transient is not sensitive toward oxygen, but reacts rapidly with the nucleophilic chloride anion (cf. eq 3 and inset a in Figure 1), forming trityl chloride. The rate constant of the neutralization reaction was found to be at the diffusion-controlled limit, $k_3 = 1.5 \times 10^{10}$ dm^3 mol^{-1} s^{-1}.

$$Ph_3C^+ + Cl^- \rightarrow Ph_3CCl \quad (3)$$

The question remained, to which species the absorption band with λ_{max} at 660 nm should be assigned. The species absorbing at this wavelength decay completely within 1 μs (cf. Figure 2).

The decay of this transient proceeds in an accelerated manner upon addition of Cl^- (diffusion-controlled process, $k_4 = 1.2 \times 10^{10}$ dm^3 mol^{-1} s^{-1}). It clearly indicates the ionic nature of the intermediate. Taking into account the relatively short lifetime of this transient and the pronounced effect of nucleophiles on its decay kinetics, it was interpreted to be the solute radical cation 2-NpSCPh$_3^{\bullet+}$.

$$\text{2-NpSCPh}_3^+ + \text{C1}^- \rightarrow \text{products} \quad (4)$$

The weak absorption band at 500 nm corresponds to the thionaphtyl radical 2-NpS$^{\bullet}$, as concluded from experiments with quenchers (oxygen and $Bu_4N^+Cl^-$) and by comparison with the reference spectrum of 2-thionaphtyl radical.[6]

Spectra given in Figure 1 evidence the simultaneous and prompt formation of a distinct part of both fragmentation products ($Ph_3C^{\bullet}$ and Ph_3C^+) immediately after the electron pulse. However, there is also a certain portion of fragmentation products formed in a delayed manner. The kinetics of their formation is in good accordance with the decay of the solute radical cations 2-NpSCPh$_3^{\bullet+}$. This observation is visualized by the kinetic simulation of the experimental time profile taken at 420 nm (Figure 3). So, using the program ACUCHEM[23] in a modified version,[4] a system of differential equations has been solved derived from the assumed reaction mechanism; cf. Scheme 1.

The extinction coefficients at distinct wavelengths of both trityl transients (radical and cation) are known from the literature.[21,22] The decrease in the signal amplitude at 420 nm

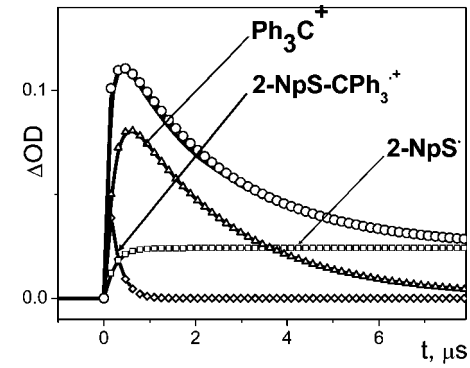

Figure 3. Time profile taken at 420 nm, showing the correlation between kinetic simulation and experimental data: (-) experimental time profile, (○) simulated composite time profile, (Δ) simulated triphenylmethyl radical cation, (□) simulated 2-thionaphtyl radical, and (◊) simulated radical cation of 2-NpSCPh$_3$.

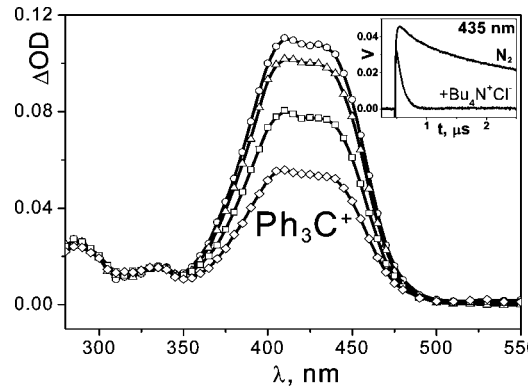

Figure 4. Transient optical absorption spectra obtained in the pulse radiolysis of N_2-saturated solution of PhOCPh$_3$ (2×10^{-3} mol dm^{-3}) in BuCl. Spectra correspond to times (○) 150 ns, (Δ) 300 ns, (□) 740 ns, and (◊) 1.7 μs after the pulse. Experimental time profiles taken at 435 nm in the absence and presence of 4×10^{-4} mol dm^{-3} $Bu_4N^+Cl^-$ are given as inset.

(absorption maximum of trityl cation) observed in the presence of $Bu_4N^+Cl^-$ is proportional to the concentration of Ph_3C^+. Accordingly, lowering of the signal amplitude at 335 nm (absorption maximum of trityl radical) induced by oxygen is proportional to the concentration of $Ph_3C^{\bullet}$. On this basis, the product ratio can be easily calculated. The product ratio of trityl fragments formed in the radiolysis of 2-naphtyltriphenylmethyl sulfide has been found to be 65% of Ph_3C^+ versus 35% of $Ph_3C^{\bullet}$.

Ionization of Triphenylmethyl Phenyl Oxide. Figure 4 shows transient absorption spectra obtained in the pulse radiolysis of a 2×10^{-3} molar solution of triphenylmethyl phenyl oxide (PhOCPh$_3$) in *n*-butyl chloride.

150 ns after the pulse, three absorption bands with λ_{max} at 280 nm, at 335 nm, and an intense peak at 420−440 nm are visible (cf. Figure 4). The latter absorption band is caused by the trityl cation Ph_3C^+. In the presence of $Bu_4N^+Cl^-$, the transient absorption at 420−440 nm was completely quenched within a few hundreds of nanoseconds (cf. eq 3 and inset in Figure 4). Under these conditions, the residual spectrum was caused exclusively by radical species (cf. Figure 5, (□) 570 ns after the pulse), since trityl cations reacted rapidly with chloride ions.

Because of the sensitivity toward oxygen the small peak at 335 nm was assigned to the trityl radical. The absorption band at 280 nm and a minor peak at 400 nm were not influenced by oxygen nor by chloride ions. Moreover, localization of these absorption maxima and the relative ratio between them cor-

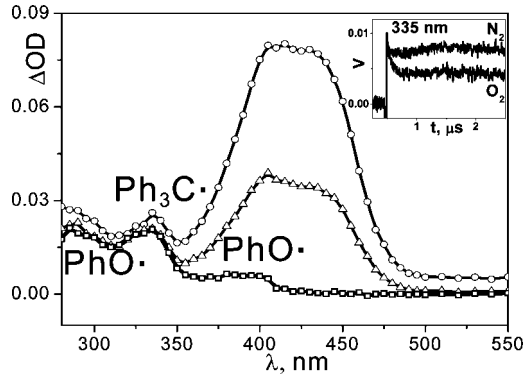

Figure 5. Transient optical absorption spectra obtained in the pulse radiolysis of N_2-saturated solution of $PhOCPh_3$ (2×10^{-3} mol dm^{-3}) upon addition of 4×10^{-4} mol dm^{-3} $Bu_4N^+Cl^-$ in BuCl. Spectra correspond to times (○) 46 ns, (Δ) 140 ns, and (□) 570 ns after the pulse. The inset shows the influence of oxygen on the transient absorption at 335 nm.

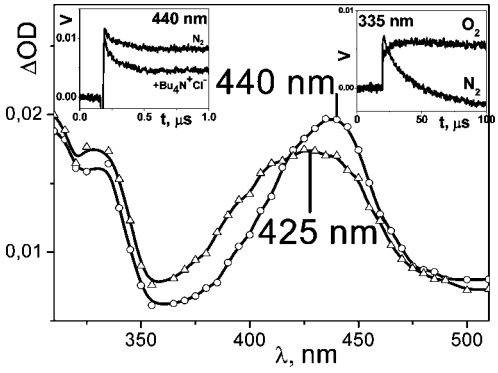

Figure 6. Transient optical absorption spectra obtained in the pulse radiolysis of N_2-saturated solution of $PhNHCPh_3$ (2×10^{-3} mol dm^{-3}) in *n*-BuCl. Spectra correspond to times (○) 100 ns, (Δ) 1.7 μs after the pulse. Insets show the influence of oxygen on transient absorption at 335 nm and influence of $Bu_4N^+Cl^-$ on transient absorption at 440 nm.

respond well with absorption bands of the phenoxyl radical observed in pulse radiolysis of phenol in *n*-butyl chloride solution.[4] Therefore, this transient was assigned to the phenoxyl radical PhO•. The product ratio, calculated as described in a previous chapter, was about 90% of Ph_3C^+ vs 10% of $Ph_3C^•$.

FET Involving Triphenylmethyl Phenyl Amine. The photodissociation of triphenylmethyl phenyl amine, among other *N*-(triphenylmethyl)anilines, was extensively studied by Siskos at al.[24] Upon photolysis in various solvents, this aromatic amine undergoes C−N bond homolysis producing triphenylmethyl radicals in a monophotonic process. Under biphotonic conditions, however, heterolytic cleavage gains importance, resulting in the formation of the triphenylmethyl cation.

We have carried out pulse radiolysis experiments with $PhNHCPh_3$ in *n*-BuCl and, in contrast to the laser flash photolysis experiments,[24] none of the trityl transients were observed (Figure 6).

As is typical for radical cationic species, in the presence of Cl^- a part of the absorption at 440 nm was quenched (cf. inset in Figure 6). However, about 50% of the signal amplitude remained. This evidence a strong superposition of two different transients, namely, a relatively short-living transient with λ_{max} at 440 nm and a long-living intermediate with λ_{max} shifted to 425 nm.

The short-living transient, formed immediately after the pulse, exhibits different kinetics as previously observed for trityl

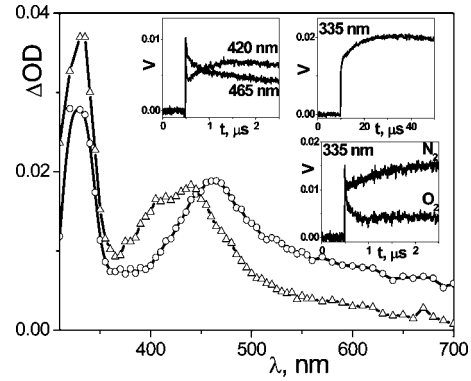

Figure 7. Transient optical absorption spectra obtained in the pulse radiolysis of N_2-saturated solution of $PhN(Me)CPh_3$ (5×10^{-3} mol dm^{-3}) in *n*-BuCl. Spectra correspond to times (○) 100 ns and (Δ) 900 ns after the pulse. Some experimental time profiles are given as insets.

cations, cf. the former examples of $2\text{-}NpSCPh_3$ and $PhOCPh_3$. Therefore, we assign these species to the metastable solute radical cations $PhNHCPh_3^{•+}$ formed in reaction 5.

$$PhNHCPh_3 + BuCl^{•+} \rightarrow PhNHCPh_{3\ metastable}^{•+} + BuCl \quad (5)$$

The long-living transient at 425 nm appears in the spectral range where normally absorption of aromatic aminyl radicals is observed.[7] Therefore, this transient is classified as an N-centered radical, which is formed via two channels: rapid deprotonation of the unstable conformer (eq 6a) and delayed deprotonation (eq 6b) of the metastable radical cation $PhNHCPh_3^{•+}$ assisted by the nucleophiles.

$$PhNHCPh_{3\ twisted}^{•+} \rightarrow PhN^•CPh_3 + H^+(BuCl) \quad (6a)$$

$$PhNHCPh_{3\ metastable}^{•+} + Cl^- \rightarrow PhN^•CPh_3 + HCl \quad (6b)$$

The absorption band at 335 nm was also attributed to aminyl radicals formed in reactions 6a and 6b). In the presence of oxygen on the long time scale, the formation of a stable product is visible (cf. inset in Figure 6), which has been identified as a nitroxyl radical,[7] in accordance with following reaction sequence

$$Ph(CPh_3)N^• + O_2 \rightarrow Ph(CPh_3)NOO^• \quad (7a)$$

$$2Ph(CPh_3)NOO^• \rightarrow 2Ph(CPh_3)NO^• + O_2 \quad (7b)$$

Pulse Radiolysis of *N*-Methyl-*N*-Triphenylmethylaniline. Ionizing a 5×10^{-3} molar solution of $PhN(Me)CPh_3$ in *n*-butyl chloride, the transient spectra shown in Figure 7 were obtained. The direct product of the electron transfer from $PhN(Me)CPh_3$ to *n*-$BuCl^{•+}$ is the amine radical cation which exhibits an absorption band with λ_{max} at 465 nm (cf. Figure 7). This looks similar as those of *N*,*N*-dimethylaniline radical cation (λ_{max} = 470 nm) obtained by Maroz et al.[7] Apart from the solute radical cation, two other transients are observed with λ_{max} at 335 and 440 nm. Their formation kinetics is related to the decay of the metastable amine radical cations (cf. insets in Figure 7) as indicated by the isosbestic point at 450 nm.

It has been observed that upon oxygen saturation only the band at 335 nm was strongly affected (cf. inset in Figure 7). The rate constant of the reaction with oxygen was estimated to be $k_9 = 1.4 \times 10^9$ dm^3 mol^{-1} s^{-1}, typical for the carbon-centered radicals. As possible structures, the triphenylmethyl radical $Ph_3C^•$, the fragmentation product of the solute radical cation or an alkyl radical, formed by deprotonation of the methyl group, should be considered.

$$Ph(CPh_3)N\text{-}CH_3^{\bullet+} + Cl^- \rightarrow Ph(CPh_3)N{-}CH_2^{\bullet} + HCl \quad (8)$$

As reported in the literature, a reaction analogous to reaction 8 was observed for tertiary amine radical cations.[7,25] Moreover, the kinetics of the reaction with oxygen evidence the structure $Ph(CPh_3)N{-}CH_2^{\bullet}$ instead of the triphenylmethyl radical for the transient absorbing at 335 nm.

$$Ph(CPh_3)N{-}CH_2^{\bullet} + O_2 \rightarrow Ph(CPh_3)N{-}CH_2OO^{\bullet} \quad (9)$$

Furthermore, according to reaction 8, after addition of $Bu_4N^+Cl^-$ to the studied solution the yield of the transients absorbing at 335 nm should be increased. Indeed, such an effect is observed (cf. Figure 8 and inset there).

By comparing the spectra given in Figure 7 and Figure 8, it can be noted that intermediates absorbing at 440 nm and at 465 nm are also affected by the addition of $Bu_4N^+Cl^-$. Thus, the decay of the solute radical cation $Ph(CPh_3)N\text{-}CH_3^{\bullet+}$ becomes significantly faster and the intermediate absorbing at 400−450 nm is not formed.

At longer times, the absorption in the region 400−450 nm appears even at low concentrations of $Ph(CPh_3)N\text{-}CH_3$, and neither kinetics nor amplitude of the signals depend on the variation of the amine concentration. This observation allows us to exclude formation of a dimer radical cation (charge transfer complex), which has been reported for some arene radical cationic structures.[26,27]

The shape of the peak allows only one cationic transient to cause the absorption at 400−450 nm, namely, trityl cation Ph_3C^+, formed in a delayed manner as a result of the asymmetric bond rupture in the metastable solute radical cation, cf. reaction 10.

$$Ph(CPh_3)N{-}CH_{3\ metastable}^{\bullet+} \rightarrow PhN^{\bullet}CH_3 + {}^+CPh_3 \quad (10)$$

Ionization of 1,1,1,2-Tetraphenylethane (Benzyltriphenylmethane). Upon ionization of benzyl triphenyl methane $PhCH_2CPh_3$, the appearance of the solute radical cation cannot be detected because of its short lifetime. Instead, only fragmentation products are observed (Figure 9).

The intense twin peak with a maximum in the range 420−450 nm was attributed to the trityl cation Ph_3C^+ as analogously described for the other electron donors in this paper. The trityl cation is promptly quenched in the presence of chloride anion (cf. eq 3 and inset in Figure 9). The counterpart of Ph_3C^+, i.e., the benzyl radical[28] $PhCH_2^{\bullet}$, is responsible for the absorption band with λ_{max} at 315 nm. When the measurements are

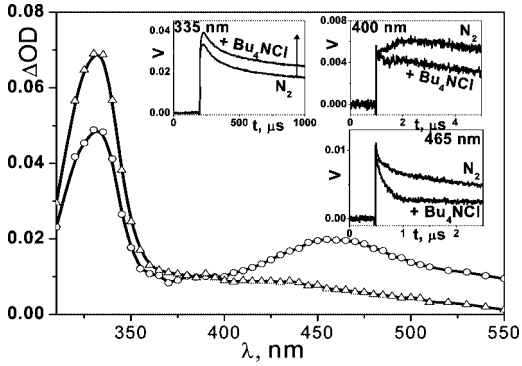

Figure 8. Transient optical absorption spectra obtained in the pulse radiolysis of N_2-saturated solution of $PhN(Me)CPh_3$ (5×10^{-3} mol dm^{-3}) upon addition of 1×10^{-3} mol dm^{-3} $Bu_4N^+Cl^-$ in *n*-BuCl. Spectra correspond to times (○) 60 ns and (Δ) 1.3 μs after the pulse. Insets show the influence of $Bu_4N^+Cl^-$ on transient absorption at 335, 400, and 465 nm.

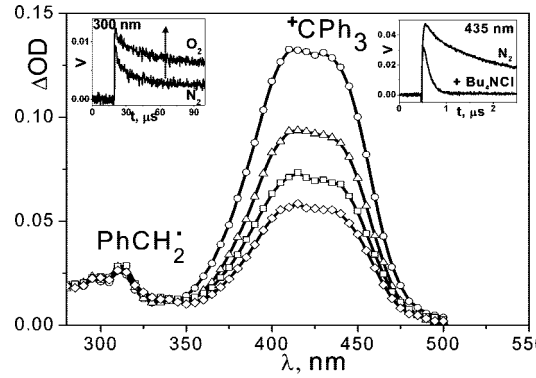

Figure 9. Transient optical absorption spectra obtained in the pulse radiolysis of N_2-saturated solution of $PhCH_2CPh_3$ (2×10^{-3} mol dm^{-3}) in *n*-BuCl. Spectra correspond to times (○) 100 ns, (Δ) 500 ns, (□) 1.0 μs, and (◊) 1.5 μs after the pulse. Insets show the influence of $Bu_4N^+Cl^-$ and O_2 on the transient kinetic behavior at distinct wavelengths.

conducted in oxygen-saturated solution, a strong increase in the absorbance in the UV region of the spectrum is observed, cf. inset in Figure 9. This effect is caused by the formation of alkylperoxy radicals: $PhCH_2OO^{\bullet}$ and *n*-$BuOO^{\bullet}$ (*n*-$Bu^{\bullet}$ are formed as a product of the solvent radiolysis); see reactions 11 and 12.[29]

$$PhCH_2^{\bullet} + O_2 \rightarrow PhCH_2OO^{\bullet} \quad (11)$$

$$n\text{-}Bu^{\bullet} + O_2 \rightarrow n\text{-}BuOO^{\bullet} \quad (12)$$

The experimental data presented above clearly indicate the existence of only one fragmentation channel for the solute radical cation $PhCH_2CPh_3^{\bullet+}$, leading to the formation of benzyl radicals and trityl cations:

$$PhCH_2CPh_3 + BuCl^{\bullet+} \rightarrow [PhCH_2CPh_3]^{\bullet+} + BuCl \rightarrow PhCH_2^{\bullet} + CPh_3^+ + BuCl \quad (13)$$

Discussion

Time Scale and Sequence of the FET Events. As already indicated in Scheme 1, the gross reaction of FET (reaction 1b), although looking as an elementary process, can be reasonably split into several single steps by analyzing the kinetic time profiles of the solvent radical ions as well as the product intermediates:

$$RX^{\bullet+} + D \underset{\text{diffusion}}{\rightleftharpoons} RX^{\bullet+}\ldots D \underset{\text{e-jump}}{\rightleftharpoons} RX\ldots D^{\bullet+} \underset{\text{diffusion}}{\rightleftharpoons} RX + D^{\bullet+} \quad (14)$$

In the nonpolar environment, the ionic species are very weakly solvated. The interaction between the electron donor molecule and the solvent parent radical cation, i.e., the real electron jump, takes place within the first encounter in an unhindered manner. This is conditioned by a large difference in the ionization potentials between reaction partners and by the negligible solvation effect. The electron jump occurs in the subfemtosecond time domain, whereas molecular oscillations take place in the femtosecond time range. Hence, the geometry and, consequently, the electron distribution in the ionized molecule (i.e., radical cation) preserves the same configuration as in the ground state. This leads to the formation of two types of radical cations with very different properties: (a) a metastable radical cation with optimal delocalization of spin over the whole

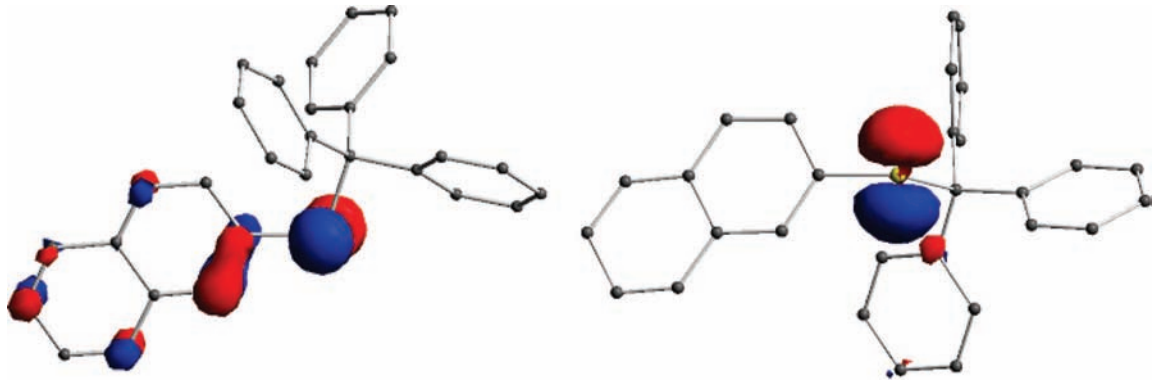

Figure 10. Electron distribution in the HOMO for the ground state of 2-NpSCPh$_3$ in the planar (left-hand side) and twisted (right-hand side) conformation. H atoms are omitted.

aromatic system and (b) a fragmentizing, dissociative type of radical cations with dominant localization of the unpaired electron, e.g., at the heteroatom. The latter intermediate is extremely unstable and undergoes fragmentation immediately after its formation. The described situation is valid for the simple organic compounds consisting of an aromatic moiety and mobile, freely oscillating polar substituents like the −OH or −NH$_2$ group. As a peculiar and very special factor determining the stability of the radical cation in such a rapid unhindered process as FET, the conformational state of the molecule in the moment of ionization has to be mentioned, which is directly connected with the electron distribution within the molecule.

The gross reaction of FET is governed by diffusion and, consequently, needs nanoseconds to proceed. Therefore, diffusion limits the experimental observation to the nanosecond time domain. The electron jump, however, is by far the fastest step of FET.[30] It is completed within less than a femtosecond. On the femtosecond time scale, the intramolecular motions like rotation (torsion) and vibration take place. The dissociation of the unstable twisted radical cation is likely to happen during the first vibration of the corresponding bond.[3] Otherwise, relaxation into the planar state and energetic optimization would happen.

Pulse radiolysis with nanosecond time resolution enables the direct observation of the diffusion-controlled gross process and of the delayed decay of the metastable radical cations. Hence, it enables one to distinguish between two direct products of the FET.

Interpretation of the Fragmentation Pattern after FET. The ionization of the different trityl derivatives in nonpolar media described in this paper seems to be an interesting case as far as the studies of the stability of the radical cations formed in FET are concerned. The asymmetric radical cations derived from these compounds are able to undergo bond rupture with the subsequent formation of two alternative couples of radical and cationic species. It is known that a cation is preferably formed from the fragment with the lower ionization potential under the condition that the thermodynamic equilibrium is established.[31] This empiric rule seems to be invalid for such an exergonic process as FET, for which thermodynamically unfavorable products are often detected (cf. preceding paragraphs). Herein, crucial factors affecting the fragmentation pattern of the solute radical cations generated in the FET process giving rise to the radical and cationic parts are defined and analyzed.

If the rotational barrier E_a in the ground state is relatively small (as will be shown further on, this is a case for all the studied compounds), then the internal rotation around the heteroatom − CPh$_3$ bond proceeds in an unrestricted manner. Therefore, in the ground state all the studied compounds exist as a variety of all possible rotational conformers. These conformers are characterized by different electron distribution, depending on the angle of twist of the substituent toward the aromatic ring. Upon ionization in a nonpolar environment, the free electron transfer occurs as a single, very fast electron jump. According to the Born−Oppenheimer approximation, the molecular geometry remains unchanged on the time scale when a fast (vertical) electron jump and an electron relaxation process take place. Thus, the generated radical cations inherit the geometry of the parent ground-state molecules.

Let us have a closer look at the example of 2-naphtyltriphenylmethyl sulfide. This compound attracts special attention since its ionization in *n*-butyl chloride solution allows the direct detection of the solute radical cation 2-NpSCPh$_3^{\bullet+}$ and of the alternative products of its subsequent fragmentation—Ph$_3$C$^\bullet$, Ph$_3$C$^+$, and 2-NpS$^\bullet$. In fact, the sum of the rotational conformers produced in the course of the intramolecular rotation around 2-NpS−CPh$_3$ bond in the ground state is not uniform. On the basis of the angle of twist, i.e., location of the -CPh$_3$ group with respect to the naphthalene moiety, as a simplification, the mixture of rotational conformers can be divided into two fractions. These fractions refer to the extreme conformational arrangements of the donor molecule, namely, planar and twisted. The planar type represents all molecules with the aromatic ring (naphthalene moiety in the case of 2-NpSCPh$_3$) positioned approximately in the same plane as the aliphatic carbon atom of the trityl group. In this conformation, the best overlap between the aromatic π-system and the electrons of the heteroatom is achieved. In contrast, the twisted type refers to all the structures with the strongly twisted bulky trityl substituent toward the aromatic ring. The twisted conformation disables the delocalization of the electrons of the heteroatom with in the naphthalene aromatic moiety. To demonstrate this electronic effect, the electron distribution of the two extreme conformations (planar and twisted) in the HOMO level (also n-orbital) are shown in Figure 10. Although none of these confirmations really stand for the sterically preferred structures, the figure demonstrates extremes in the electron distribution in the ground state.

As was mentioned before, after the fast electron jump the radical cations are produced with the geometry (and electron distribution) of their ground-state precursors. Hence, the spin density in the twisted radical cation is mostly localized on the heteroatom and partially on the benzene rings of the trityl fragment, whereas in the planar conformers spin is more efficiently distributed between the heteroatom and the naphthalene aromatic moiety. Therefore, the planar type of the

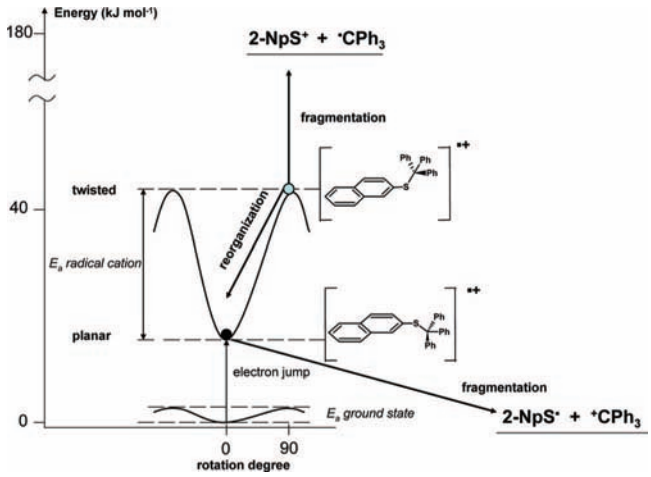

Figure 11. Potential energy diagram describing energetic profiles of the planar and twisted radical cation conformers and subsequent fragmentation reactions.

asymmetric radical cation tends to follow the thermodynamically favorable fragmentation pattern, i.e., it fragments into trityl cations and the corresponding heteroatom-containing radicals. Contrarily, the decay of the twisted type of the transient occurs within the first vibrational motion and generates trityl radicals and cations derived from the counterpart of the molecule. These products are not favored thermodynamically.

Planar donor radical cations are not in each case stable enough to be observed in the nanosecond spectroscopy. Nevertheless, even if they exhibit lifetimes of $\leq$10 ns we specify them as metastable, as done in the case of $PhSCPh_3^{\bullet+}$; see ref 20. In contrast, the twisted solute radical cation $PhSCPh_3^{\bullet+}$ is called unstable (or dissociative). This terminology is justified as far as relative energies and lifetimes of the different conformers of the radical cation are concerned. Thus, the twisted conformer type is placed on the top of the potential energy surface, whereas the planar radical cation is located at the minimum energy point on the potential energy curve; see also Figure 11. Hence, the unstable or dissociative radical cations are derived from the twisted conformer type and their fragmentation takes place in the femtosecond time domain, whereas the metastable radical cations are formed from the planar conformer type and undergo fragmentation in the nanosecond time range. The dissociative type of the radical cations is a characteristic product of the FET.

There is a significant difference in the ionization potentials between the trityl radical and the counterpart of the studied molecules. For example, in the case of $PhOCPh_3$ this difference amounts to 1.24 eV ($IP_{PhO\bullet} - IP_{Ph3C\bullet} = 8.50$ eV[32] $- 7.26$ eV[21]). Such an energy gap should result in the exclusive formation of phenoxyl radicals $PhO^{\bullet}$ and trityl cations Ph_3C^+ as its counterpart. In turn, the alternative fragmentation pattern should be completely disabled. Nevertheless, a distinct fraction (about 10%) of thermodynamically unfavorable trityl radical $Ph_3C^{\bullet}$ is also formed. This fact might be explained if the alternative fragmentation patterns are assumed to not originate from a common precursor, solute radical cation, but from different types of this radical cation, namely, its planar and twisted conformers. Because of the dramatically increased rotational barrier in the ionized state, the planar conformer type of the radical cation cannot convert into the twisted one. Thus, the different conformer state and the correspondingly different electron distribution in two extreme arrangements results in two independent fragmentation channels, giving rise to alternative couples of fragmentation products. But certainly, a distinct part of the twisted radical cation can undergo relaxation into the planar conformation with minimum energy.

Interpretation Supported by Quantum Chemical Calculations. Since the intramolecular dynamic processes were proved to be of deciding importance in the mechanism of the FET, the experimental data on the ratio between trityl radical and trityl cation appearing as the alternative products of the solute radical cation fragmentation are given in comparison with quantum chemically calculated parameters, obtained by the density functional theory (DFT) B3LYP/6$-$31G(d)[33] method. One of them is the bond dissociation energy for the cleavage of $ArX-CPh_3$ bond (where X is the heteroatom) in the solute radical cation leading to two possible pairs of fragments: (i) $ArX^{\bullet}$ and Ph_3C^+ and (ii) ArX^+ and $Ph_3C^{\bullet}$. The fragmentation pattern depends on the position of the trityl group toward benzene or naphthalene ring (twisted vs planar conformation). The activation energy E_a for the rotation around the $ArX-CPh_3$ bond was calculated for the ground and radical cation states. This manifold of data is summarized in Table 1.

As can be seen from data presented in Table 1, there are several parameters that are similar for all the studied compounds. First, all the molecules in the ground state exhibit free rotation around the heteroatom$-CPh_3$ bond, since the value of the rotational barrier E_a is quite low, i.e., less than 20 kJ mol^{-1}. However, after ionization a significant increase of E_a occurs. Benzyltriphenylmethane is the only exception from this rule. For this compound, even in the radical cation state rotational motion is almost unrestricted ($E_a = 18.8$ kJ mol^{-1}).

Another important issue concerns the energetic aspects of the fragmentation of the solute radical cation into alternative pairs of products. The fragmentation channel leading to the formation of trityl radical $Ph_3C^{\bullet}$ and countercation ArX^+ is highly endothermic for all the studied substances. Dissociation into trityl cations Ph_3C^+ and the corresponding radicals $ArX^{\bullet}$ is calculated to be an exothermic process for $PhCH_2CPh_3^{\bullet+}$, $PhOCPh_3^{\bullet+}$, and 2-$NpSCPh_3^{\bullet+}$ radical cations, whereas for both amine radical cations, namely, $PhNHCPh_3^{\bullet+}$ and Ph-$N(Me)CPh_3^{\bullet+}$, this process is endothermic.

After ionization, the rotational barrier E_a restricts only the transformation of the planar conformer into the twisted one, whereas the reorganization of the twisted structure into the planar one (with minimum energy) is not hindered. E_a shows the difference in the energetic profiles between the twisted and the planar structures of the radical cation (cf. Figure 11). Hence, this parameter can be considered a factor of destabilization of the twisted radical cation. Indeed, a high rotational barrier enables a very rapid (in the femtosecond time range) fragmentation of the twisted, dissociative solute radical cation according to the thermodynamically unfavorable pathway, in which the trityl radical is formed as product. This is demonstrated on the examples of triphenylmethyl phenyl oxide ($E_a = 29.3$ kJ mol^{-1}) and 2-naphtyl triphenylmethyl sulfide ($E_a = 43.9$ kJ mol^{-1}). Under these circumstances (high E_a), the transformation of the planar radical cation into the twisted one becomes impossible. Highly destabilized radical cations in the twisted conformation tend to decay via an energetically unfavorable channel producing $Ph_3C^{\bullet}$ and corresponding ArX^+. This fragmentation, however, has to compete with the structural relaxation of the twisted radical cation into the energetically preferable planar geometry.

Although the energy gap between the twisted radical cation and the reaction channel yielding the trityl radical is rather vast (cf. Table 1), the possibility of such a fragmentation is justified by a kinetic factor. Quantum chemically calculated frequencies

TABLE 1: DFT Calculated Quantum Chemical Parameters and Experimental Data on the Yields of Trityl-Derived Transients

	Bond dissociation energy, E_{diss} (kJ mol^{-1})		Ratio between fragmentation channels		Rotational barrier, E_a(kJ mol^{-1})	
	ArX^+/ $Ph_3C^\bullet$	$ArX^\bullet$/Ph_3C^+	Ph_3C^+	$Ph_3C^\bullet$	ground state	radical cation
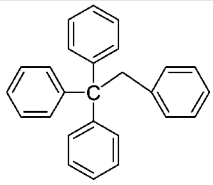	96	-19	100%	0%	2.0	18.8
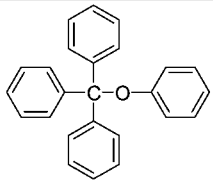	233	-26	90%	10%	5.9	29.3
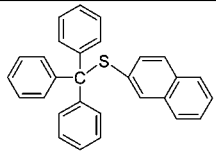	176	-10	65%	35%	4.2	43.9
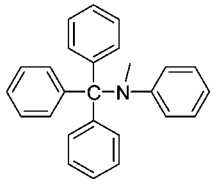	172	16	<5%	*	2.5	48.5
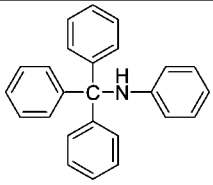	257	61	0%	*	16.7	35.9

* Deprotonation instead of C−N bond cleavage.

and times of rotational and vibrational motions of various bonds important for the FET mechanism are shown in Table 2. As can be seen, vibrational motions proceed with frequencies, which are more than 1 order of magnitude higher compared to rotational ones. So, the solute radical cation in the twisted conformation dissociates into $Ph_3C^\bullet$ and ArX^+ within the first vibrational motion.

Moreover, two further aspects should be taken into account: first, the affinity of the *n*-BuCl to the generated cationic species (ArX^+), which decreases the energy of these products in comparison to the gas phase conditions; second, the FET is a very exothermic process taking place in one step. Such processes generate vibrationally excited states of the products.[34] An excess energy, owned by the transients in the vibrationally excited states, contributes to overcoming of the energetic gap between

TABLE 2: Quantum Chemically Calculated Rotational and Vibrational Frequencies and Times, Energy of Vibrational Motion[a]

solute	ν_{rot}, cm^{-1}	t_{rot}, fs	ν_{vib}, cm^{-1}	E_{vib}, kJ mol^{-1}	t_{vib}, fs
PhO−CPh_3	76	440	1007 (O-CPh_3)	12	33
PhNH−CPh_3	71	471	1053 (N-CPh_3)	13	32
			3591 (N−H)	44	9
PhN(Me)−CPh_3	31	1079	990 (N-CPh_3)	13	34
			3013 (C−H in CH_3)	36	11
$PhCH_2$−CPh_3	40	836	1017 (C−C)	12	33
			3060 (C−H in CH_2)	37	11
2-NpS−CPh_3	24	1393	841 (S-CPh_3)	10	40

[a] Chemical bonds involved into oscillation are given in the brackets.

the twisted radical cation and the reaction channel producing trityl radicals or other thermodynamically unfavorable products. Thus, the high energy of vibrational motion (cf. Table 2) for the N−H and C−H bond in PhNH-CPh_3 and PhN(Me)-CPh_3, correspondingly, is assumed to facilitate thermodynamically unfavorable fragmentation patterns.

The efficiency of the energetically unfavorable fragmentation channel depends on the amplitude of the rotational barrier. If the activation energy of the rotation E_a is higher than 20 kJ mol^{-1}, then a distinct part of twisted conformers is destabilized enough to fragmentize, yielding trityl radicals. Nevertheless, a considerable part of the twisted rotational conformers has a chance to relax into the planar structure and, hence, to escape from the thermodynamically unfavorable scenario of fragmentation. Thus, the rotational barrier E_a affects the ratio between the alternative fragmentation pathways of the solute radical cation.

Finally, the FET behavior of the studied amines $PhNHCPh_3$ and $PhN(Me)CPh_3$ should be discussed. From the bond dissociation energies (Table 1), for both amines any type of the N−C bond cleavage is endothermic. Nevertheless, for Ph-N(Me)CPh_3 the fragmentation pathway leading to the trityl cation and corresponding $ArX^{\bullet}$ radical (reaction 10) is only slightly endothermic (E_{diss} = 16 kJ mol^{-1}) and, in principle, can take place. The efficiency of this reaction channel was estimated to be less than 5%. However, the major part of the solute radical cations derived from the studied amines prefers to undergo the nucleophile or the solvent-assisted deprotonation (cf. reactions 6a, 6b, and 8). Such behavior is governed by several factors such as the following:

(1) endothermic values for the N−C bond rupture (cf. Table 1).

(2) high values of the rotational barrier E_a and, therefore, strong destabilization of the twisted conformers.

(3) higher frequency of the vibrational motions compared to the rotational ones (cf. Table 2) which, subsequently, leads to the deprotonation within the first vibrational motion.

The processes studied in this paper are generalized in the reaction Scheme 2 (amines are not included). The experimentally observed transients are bold-faced.

Process (1) in Scheme 2 corresponds to the diffusional approach of the reactants (rate-determining step of the FET). An unhindered electron jump (2) in the first encounter of the partners creates the radical cations with preserved geometry (and electron distribution) of their molecular precursors. Depending on the angle of twist of the trityl group toward the aromatic moiety, two extreme conformer types are defined: (a) planar radical cation placed in the minimum on the potential energy surface and (b) twisted radical cation destabilized by the strongly increased value of the activation energy (E_a) for the rotation in the ionized state.

Planar and twisted types of the donor radical cation have significantly different electron distribution. The energy difference between them is characterized by the increased activation energy (E_a) for the rotation, which plays a deciding role in their subsequent fragmentation. Thus, the metastable radical cation (3), which corresponds to the planar conformation, follows the thermodynamically favorable pathway of dissociation generating $ArX^{\bullet}$ and Ph_3C^+ (4). It is also neutralized in the reaction with nucleophiles (5). In contrast, the dissociative radical cation (6), corresponding to the twisted conformation, may dissociate within the first valence vibrational motion into thermodynamically unfavorable couple of products—ArX^+ and $Ph_3C^{\bullet}$ (7). The probability of such endothermic fragmentation is determined by kinetic control. The fragmentation of the dissociative radical cation (6) competes with the relaxation (8) into a more preferable planar structure.

SCHEME 2: General Scheme of FET Involving Trityl-Containing Donors[a]

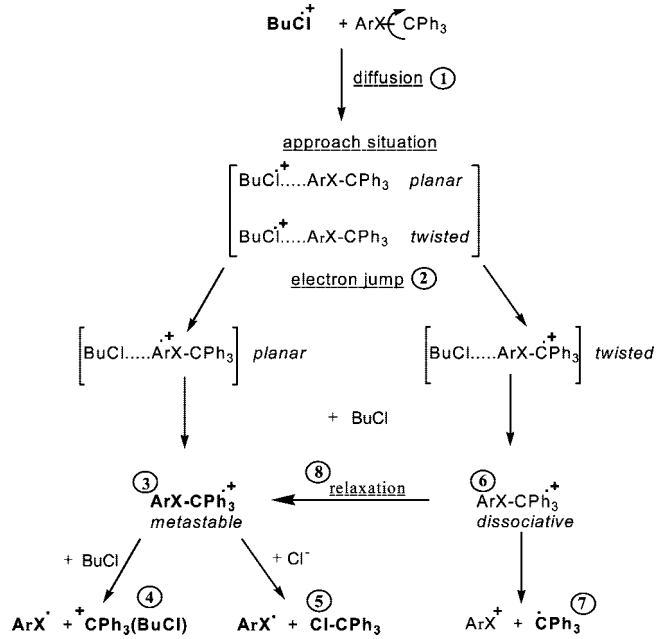

[a] Species given in bold-faced letters were directly observed in pulse radiolysis.

Conclusions

The free electron transfer (FET) from five different trityl-containing aromatic compounds to the solvent radical cation of *n*-BuCl was studied. The results fit well into the general concept of this phenomenon, i.e., they reflect femtosecond intramolecular dynamics.

The research work presented in this paper gives an extended energetic and kinetic analysis of the free electron transfer phenomenon. On the basis of the experiments presented in this work, we were able to derive the following:

(1) a complete quantitative identification of the fragmentation processes, and, therefore, the product pattern of FET.

(2) a reasonable interpretation of the product pattern supported by the energetic analysis.

(3) A general scheme of the processes regarding FET was given.

References and Notes

(1) Mehnert, R.; Brede, O.; Naumann, W. *Ber. Bunsen-Ges. Phys. Chem.* **1984**, *88*, 71.

(2) Mehnert, R.; Brede, O.; Naumann, W. *Ber. Bunsen-Ges. Phys. Chem.* **1982**, *86*, 525.

(3) Brede, O.; Naumov, S *J. Phys. Chem. A.* **2006**, *110*, 11906.

(4) Brede, O.; Hermann, R.; Naumann, W.; Naumov, S. *J. Phys. Chem. A.* **2002**, *106*, 1398.

(5) Ganapathi, M. R.; Hermann, R.; Naumov, S.; Brede, O. *Phys. Chem. Chem. Phys.* **2000**, *2*, 4947.

(6) Hermann, R.; Dey, G. R.; Naumov, S.; Brede, O. *Phys. Chem. Chem. Phys.* **2000**, *2*, 1213.

(7) Maroz, A.; Hermann, R.; Naumov, S.; Brede, O *J. Phys. Chem. A* **2005**, *109*, 4690.

(8) Brede, O.; Maroz, A.; Hermann, R.; Naumov, S. *J. Phys. Chem. A* **2005**, *109*, 8081.

(9) Mohan, H.; Hermann, R.; Naumov, S.; Mittal, J. P.; Brede, O. *J. Phys. Chem. A* **1998**, *102*, 5754.

(10) Brede, O.; Hermann, R.; Naumov, S.; Zarkadis, A. K.; Perdikomatis, G. P.; Siskos, M. G. *Phys. Chem. Chem. Phys.* **2004**, *6*, 2267.
(11) Karakostas, N.; Naumov, S.; Siskos, M. G.; Zarkadis, A. K.; Hermann, R.; Brede, O. *J. Phys. Chem. A.* **2005**, *109*, 11679.
(12) Gomberg, M. *J. Am. Chem. Soc.* **1900**, *22*, 757.
(13) Gomberg, M. *Ber. Dtsch. Chem. Ges.* **1902**, *35*, 2397.
(14) Arnett, E. M.; Flowers, R. A.; Ludwig, R. T.; Meekhof, A. E.; Walek, S. A. *J. Phys. Org. Chem.* **1997**, *10*, 499.
(15) Adam, W.; Arguello, J. E.; Penenory, A. B. *J. Org. Chem.* **1998**, *63*, 3905.
(16) Gomberg, M.; Kamm, O. *J. Am. Chem. Soc.* **1917**, *39*, 2009.
(17) Siskos, M. G.; Garas, S. K.; Zarkadis, A. K.; Bokaris, E. P. *Chem. Ber.* **1992**, *125*, 2477.
(18) Behloul, C.; Guijarro, D.; Yus, M. *Synthesis* **2004**, *8*, 1274.
(19) Beckhaus, H.-D.; Dogan, B.; Schaetzer, J.; Hellmann, S.; Rüchardt, C. *Chem. Ber.* **1990**, *123*, 137.
(20) Karakostas, N.; Naumov, S.; Brede, O. *J. Phys. Chem. A* **2007**, *111*, 71.
(21) Faria, J. L.; Steenken, S. *J. Am. Chem. Soc.* **1990**, *112*, 1277.
(22) Chu, T. L.; Weissman, S. I. *J. Chem. Phys.* **1954**, *22*, 21.
(23) Brown, W.; Herron, J. T.; Kahaner, D. K. *Int. J. Chem. Kinet.* **1998**, *20*, 51.
(24) Siskos, M. G.; Zarkadis, A. K.; Steenken, S.; Karakostas, N.; Garas, S. K. *J. Org. Chem.* **1998**, *63*, 3251.
(25) Brede, O.; Beckert, D.; Windolph, C.; Göttinger, H. A. *J. Phys. Chem. A* **1988**, *102*, 1457.
(26) Robinson, A. J.; Rodgers, M. A. J. *J. Chem. Soc., Faraday I* **1973**, *69*, 2036.
(27) Egusa, S.; Tabata, Y.; Arai, S.; Kira, A.; Imamura, M. J. *Polym. Sci., Polym. Chem. Ed.* **1978**, *16*, 729.
(28) Claridge, R.; Fischer, H. *J. Phys. Chem.* **1983**, *87*, 1960.
(29) Noziere, B.; Lesclaux, R.; Hurley, M. D.; Dearth, M. A.; Wallington, T. J. *J. Phys. Chem.* **1994**, *98*, 2864.
(30) Turro, N. J. *Modern Molecular Photochemistry*; University Science Books: Mill Valley, CA, 1991; p 6.
(31) Popielarz, R.; Arnold, D. R. *J. Am. Chem. Soc.* **1990**, *112*, 3068.
(32) Klein, E.; Lukes, V.; Cibulkova, Z.; Polovkova, J. *THEOCHEM* **2006**, *758*, 149.
(33) Becke, A. D. *J. Chem. Phys.* **1993**, *98*, 5648.
(34) Medvedev, E. S.; Osherov, V. I. *Radiationless Transitions in Polyatomic Molecules*; Springer Series in Chemical Physics 57; Springer: Berlin, 1995, p 36.

JP8053982